

Orbital Angular Momentum and Spectral Flow in Two Dimensional Chiral Superfluids

Yasuhiro Tada,¹ Wenxing Nie,^{2,1,*} and Masaki Oshikawa¹

¹*Institute for Solid State Physics, The University of Tokyo, Kashiwa 277-8581, Japan*

²*Institute for Advanced Study, Tsinghua University, Beijing 100084, China*

We study the orbital angular momentum (OAM) L_z in two dimensional chiral $(p_x + ip_y)^\nu$ -wave superfluids (SF) of N fermions on a disc at zero temperature, in terms of spectral asymmetry and spectral flow. It is shown that $L_z = \nu N/2$ for any integer ν , in the BEC regime. In contrast, in the BCS limit, while the OAM is $L_z = N/2$ for the $p+ip$ -wave SF, for chiral SF with $\nu \geq 2$, the OAM is remarkably suppressed as $L_z = N \times O(\Delta_0/\varepsilon_F) \ll N$, where Δ_0 is the gap amplitude and ε_F is the Fermi energy. We demonstrate that the difference between the $p+ip$ -wave SF and the other chiral SFs in the BCS regimes originates from the nature of edge modes and related depairing effects.

PACS numbers: 67.30.H-,74.20.-z

The orbital angular momentum (OAM) L_z of chiral superfluids (SF) of fermions is a fundamental problem which has been under intense investigation over several decades [1–21]. Among the chiral SFs, the simplest $p+ip$ -wave pairing state describes the A-phase of liquid ³He [1], and quite likely also the superconducting phase of Sr₂RuO₄ [22, 23]. The OAM is a direct manifestation of the broken chiral symmetry [24], and is also closely related to the edge current, which has been so far not observed experimentally in Sr₂RuO₄ despite the expectation from the $p+ip$ -wave SF picture [25].

Most of the existing studies on the OAM have focused on $p+ip$ -wave SF. However, higher-order chiral SFs such as $d+id$, $f+if$, ...-wave ones are also of interest [26, 27], and have potential applications to candidates for chiral superconductors, such as UPt₃ [28], URu₂Si₂ [29], and SrPtAs [30]. We focus on fundamental chiral SFs with the pairing symmetry $\sim (p_x + ip_y)^\nu$ which can be classified by the integer angular momentum ν of each Cooper pair: $\nu = 1$ corresponds to $p+ip$, $\nu = 2$ to $d+id$, and so on. In fact, as we will demonstrate in this Letter, there is an unexpected fundamental difference between the $p+ip$ -wave and higher-order chiral SFs with respect to the OAM; thus it is essential to consider the higher-order ones as well, for a complete understanding of the problem.

The main issue with the OAM is that different viewpoints lead to different predictions for it, resulting in an apparent paradox [18]. One argument is that, since each Cooper pair has the OAM ν , $L_z = \nu N/2$ where N is the total number of fermions. There is, however, a different view starting from the normal (non-superconducting) Fermi liquid, which has $L_z = 0$. Formation of Cooper pairs with an angular momentum would change the value of L_z from zero to a non-vanishing value in the chiral SF phase. However, since only the low-energy fermions near the original Fermi surface would be affected, L_z should be suppressed as $(\Delta_0/\varepsilon_F)^\gamma N/2$ with $\gamma > 0$, where Δ_0 is the pairing gap amplitude and ε_F is the Fermi energy.

Of course, the analysis did not stop at the hand-waving arguments and many calculations have been carried out

based on various schemes, leading to different results. We note that, in the limit of strong pairing of fermions, the superfluid phase may be understood as a result of Bose-Einstein condensation (BEC) of bosonic molecules. In this limit, it would be natural to expect that $L_z = \nu N/2$, since each bosonic molecule carries the OAM ν . However, this does not necessarily imply that the same value of L_z persists in the regime where the superfluid is described by Bardeen-Cooper-Schrieffer (BCS) theory. In fact, the “weak-pairing” chiral SFs in the BCS regime is a topological superfluid with gapless edge states, while the “strong-pairing” chiral SFs in the BEC regime is a non-topological one [31]. Thus they are distinct superfluid phases separated by a quantum phase transition, and thus L_z could take very different values. Even within the same phase, the stability of the OAM has not been established.

Historically, strong reduction of L_z ($\gamma \geq 1$) was predicted for the BCS regime of $p+ip$ -wave SF, in several of the earlier papers on the subject [17–21]. On the other hand, many others, including most of more recent ones support the full OAM $L_z = N/2$ at zero temperature, even for the BCS regime [2–16]. However, so far there is no clear physical picture why $L_z = N/2$ holds even in the BCS regime. Experimental investigation of the problem is difficult and there have been very few reports so far [32, 33]. Therefore the long-standing paradox is not yet resolved even for the $p+ip$ -wave SF, let alone for the higher-order ones with $\nu \geq 2$.

In this study, we investigate the problem in the simplest ideal setting: two dimensional (2D) chiral SFs confined on a completely circular disc with a specular wall at zero temperature, in the framework of Bogoliubov-de Gennes (BdG) Hamiltonian. For simplicity, we assume that the d -vector is $\mathbf{d} = (0, 0, d_z)$ for the triplet states so that both the singlet states and the triplet states can be discussed in a parallel way; our analysis is also applicable to the spinless fermions with slight modifications. We consider the Hamiltonian $\hat{H} = \int d^2x \psi_\sigma^\dagger [(p_x^2 + p_y^2)/2m_0 + V - \mu] \psi_\sigma + \int d^2x \psi_\uparrow^\dagger \Delta(r) (p_x + ip_y)^\nu \psi_\downarrow^\dagger + (\text{h.c.})$, where

$p_j = -i\partial/\partial x_j$, m_0 is the fermion mass, and μ is the chemical potential. $V(r)$ describes the wall of the container, and is chosen to be $V(r < R) = 0$ and $V(r > R) = \infty$ with a radius R . There is no texture in this model.

Although we only consider constant pair potentials in numerical calculations, our discussion is also applicable to systems with $\Delta(r)$ for which r -dependence is determined through self-consistent calculations. The field operator is expanded in terms of a single particle basis as $\psi_\sigma(\mathbf{r}) = \sum_{nl} c_{nl\sigma} \varphi_{nl}(\mathbf{r})$ where φ satisfies $[(p_x^2 + p_y^2)/2m_0 + V(r) - \mu]\varphi_{nl} = \varepsilon_{nl}\varphi_{nl}$ [8, 10]. Then the Hamiltonian becomes

$$\hat{H} = \sum_l \sum_{nn'} \begin{bmatrix} c_{n,l+\nu,\uparrow}^\dagger \\ c_{n,-l,\downarrow} \end{bmatrix}^T \times \begin{bmatrix} \varepsilon_{n,l+\nu}\delta_{nn'} & \Delta_{nn'}^{(l)} \\ \Delta_{nn'}^{(l)*} & -\varepsilon_{n,-l}\delta_{nn'} \end{bmatrix} \begin{bmatrix} c_{n',l+\nu,\uparrow} \\ c_{n',-l,\downarrow}^\dagger \end{bmatrix}, \quad (1)$$

where $\Delta_{nn'}^{(l)} = \int \varphi_{n,l+\nu}^* \Delta(p_x + ip_y)^\nu \varphi_{n',-l}$, with an appropriate high-energy regularization. We denote the above matrix as $(H_{\text{BdG}}^{(l)})_{nn'}$. The particle-hole symmetry connects different l -sectors as $PH_{\text{BdG}}^{(l)}P^{-1} = -H_{\text{BdG}}^{(-l-\nu)*}$ where $P = \sigma_x(i\sigma_y)$ in the Nambu space for odd (even) ν , which implies that, although eigenvalues come in pairs, each of them lies in different l -sectors.

The OAM L_z corresponds to the operator $\hat{L}_z = \int d^2x \psi_\sigma^\dagger (xp_y - yp_x) \psi_\sigma$, while the total particle number operator is given as $\hat{N} = \int d^2x \psi_\sigma^\dagger \psi_\sigma$. These operators are clearly defined for the present model, and include all the possible contributions. Neither \hat{L}_z nor \hat{N} commutes with the BdG Hamiltonian (1) owing to the pairing term in the Hamiltonian, and is not conserved. Nevertheless, as pointed out in Refs. [5, 6], the combination

$$\hat{\mathcal{L}}_z \equiv \hat{L}_z - \frac{\nu}{2}\hat{N} = \sum_{nl\sigma} \left(l - \frac{\nu}{2}\right) c_{nl\sigma}^\dagger c_{nl\sigma}, \quad (2)$$

commutes with the Hamiltonian (1), and thus is a conserved quantity. Physically, $\hat{\mathcal{L}}_z$ represents the correction to the OAM with respect to its ‘‘full’’ value $\nu N/2$. If the ground state belongs to the zero eigenvalue sector of $\hat{\mathcal{L}}_z = 0$, it follows that $L_z = \nu N/2$. However, $\hat{\mathcal{L}}_z$ could take different eigenvalues in the ground state, as it is clear by considering the limit of $\Delta \rightarrow 0$, where $L_z = 0$ and $\mathcal{L}_z = -\nu N/2$ hold.

Thus the eigenvalue \mathcal{L}_z of $\hat{\mathcal{L}}_z$ in the ground state is a nontrivial quantity. In fact, it can still be calculated exactly for the Hamiltonian (1). After the Bogoliubov transformation, the ground state |GS) is simply the vacuum with respect to all the positive energy quasiparticles. The eigenvalue \mathcal{L}_z for |GS) can be obtained explicitly as

$$\mathcal{L}_z = -\frac{1}{2} \sum_l \left(l + \frac{\nu}{2}\right) \eta_l, \quad \eta_l = \sum_m \text{sgn} E_m^{(l)}, \quad (3)$$

where $\{E_m^{(l)}\}_{m \in \mathbb{N}}$ are eigenvalues of $H_{\text{BdG}}^{(l)}$, and η_l is called the spectral asymmetry [6, 34–36]. In actual calculations, we introduce a cut-off $M \gg 1$ so that indices n, n' are restricted not to exceed M . Then $H_{\text{BdG}}^{(l)}$ is represented by a $2M \times 2M$ matrix, and η_l takes only even integer values. We have verified that the results are independent of M , when M is sufficiently large. From this formula, it is clear that \mathcal{L}_z can change only when there is a spectral flow, namely some of the eigenvalues of $H_{\text{BdG}}^{(l)}$ cross zero as model parameters are varied.

We first discuss the $p+ip$ -wave states ($\nu = 1$) for which the spectrum is particle-hole symmetric about $l = -1/2$:

$$\{E_m^{(l)}\}_{m=1}^{2M} = \{-E_m^{(-l-1)}\}_{m=1}^{2M}. \quad (4)$$

For simplicity, we treat the two parameters μ and Δ independently as in Refs. [8, 10, 31] for a discussion of the spectral flow. In the BEC regime, by numerically diagonalizing $H_{\text{BdG}}^{(l)}$, we obtain fully gapped spectrum as shown in Fig. 1(a), and find that the spectral asymmetry η_l is zero for all l . As a consequence, $\mathcal{L}_z = 0$ and thus follows $L_z = N/2$, as expected. However, the spectrum becomes less trivial if the system is in the BCS regime. There, a single edge mode with $E_{\text{edge}}^{(l)} \propto -(l + 1/2)$ appears as seen in Fig. 1(c), reflecting the topological nature of the phase [6, 26, 27, 31]. This edge mode is particle-hole symmetric by itself, $E_{\text{edge}}^{(l)} \sim -(l + 1/2) \sim -E_{\text{edge}}^{(-l-1)}$, and is hereafter called a particle-hole symmetric (PHS) edge mode. For spatially constant, non-vanishing pair potentials, we have confirmed that $\eta_l = 0$ for all values of l , for a sufficiently large system size where the finite-size discretization of the energy levels is small compared to $\Delta_0 = k_F \Delta$ where k_F is the Fermi wavenumber. Namely, even deep inside the BCS regime, and even for a small Δ_0 , we find $\mathcal{L}_z = 0$ in the thermodynamic limit, which implies no reduction of the OAM: $L_z = N/2$ holds exactly.

A natural question arising here is why \mathcal{L}_z remains zero in the BCS regime, despite the quantum phase transition separating it from the BEC regime. Let us first consider the limit $\mu = -\infty$ with a fixed $\Delta > 0$, where $L_z = N = 0$ holds trivially. Thus we find $\mathcal{L}_z = 0$ in this limit. Increasing μ , L_z and N acquire non-zero values. However, as long as there is no gap closing, $\mathcal{L}_z = 0$ and thus $L_z = N/2$ still hold. This gives a proof for the physical expectation that $L_z = N/2$ holds throughout the BEC regime, which belong to the non-topological strong-pairing phase.

The value of \mathcal{L}_z in the BCS regime (weak-pairing phase) is more subtle, due to the presence of the quantum phase transition at $\mu = 0$ in the thermodynamic limit. At the quantum phase transition, a gap closing is expected. However, a careful examination reveals that every eigenvalue keeps its sign when μ is continuously varied from $\mu = -\infty$ to $\mu = \varepsilon_F > 0$. In fact, for the system defined on a finite disc, the gap never closes. The gap does

approach zero at the quantum critical point, and also inside the BCS regime giving rise to the gapless chiral edge mode, but only in the thermodynamic limit. The change of the eigenvalues when μ is varied is shown in Fig. 1 (d). The edge mode appears in the BCS regime, as a set of eigenstates separated from bulk states. Although it converges to the linear gapless dispersion, all the eigenvalues corresponding to the edge mode for $l \leq -1$ come off from the upper continuum of bulk eigenstates and remain positive. Likewise, all the edge mode eigenvalues for $l \geq 0$ come from the lower continuum and remain negative. Since all the eigenvalues depend continuously on μ , this is the only possible evolution to generate the PHS edge mode, under the particle-hole symmetry (4).

Although each of L_z and N changes from the trivial values $L_z = N = 0$, $\mathcal{L}_z = L_z - N/2 = 0$ is always satisfied and any correction factor like $(\Delta_0/\varepsilon_F)^\gamma$ discussed in the introduction cannot arise. We note that this is also true for a physical process where μ and Δ are simultaneously tuned to keep N constant. Our argument only relies on the formation of the PHS edge mode separated from the bulk eigenstates, which is valid for a sufficiently large system size. The conclusion of our analysis largely agrees with the recent related calculations on $p+ip$ -wave SF [10–13], but clarify why L_z is exactly given by $N/2$ even for small Δ_0/ε_F .

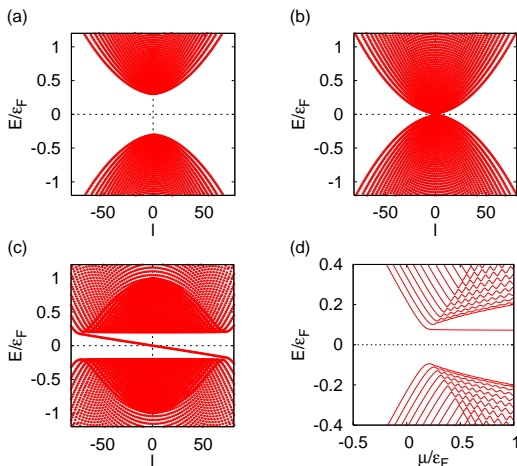


FIG. 1: Examples of spectrum in the $p+ip$ -wave SF when $k_F R = 80$, $k_F \Delta = 0.2\varepsilon_F$ for (a) $\mu = -0.3\varepsilon_F$ (BEC regime), (b) $\mu = 0$, and (c) $\mu = \varepsilon_F$ (BCS regime). (d) Evolution of the spectrum for fixed $l = -30$ as μ is changed.

Next, we move to the $d+id$ -wave states for which the spectrum is particle-hole symmetric about $l = -1$. We have numerically confirmed that $\eta_l = 0$ for all l in the BEC regime and obtain $\mathcal{L}_z = 0$, i.e. $L_z = N$. On the other hand, in the BCS states, it is known that a $d+id$ -wave state has two non-degenerate edge modes at one boundary as visualized in Fig. 2 (a) [37]. Each edge mode is particle-hole symmetric with the other branch, but not symmetric by itself; we call them non-

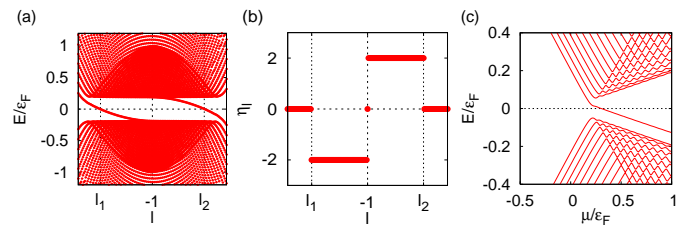


FIG. 2: Examples of (a) spectrum in the $d+id$ -wave SF and (b) the spectral asymmetry η_l for $k_F R = 80$, $k_F^2 \Delta = 0.2\varepsilon_F$, $\mu = \varepsilon_F$ (BCS regime). (c) Spectral flow for fixed $l = -30 (> l_1 = -56)$ as μ is changed.

PHS edge modes. Their dispersion relations are given as $E_{\text{edge}1,2}^{(l)} \propto -(l - l_{1,2})$, where $l_{1,2} \neq -1$ ($l_1 < l_2$) are the “Fermi angular momenta” where the edge modes cross the zero energy. The PHS of the system requires $l_1 + 1 = -(l_2 + 1)$. Interestingly, for this spectrum, we find that some of the η_l ’s become non-vanishing, as shown in Fig. 2(b): $\eta_l = 0$ for $l < l_1$, $l > l_2$, and $l = -1$, while $\eta_l = -2$ for $l_1 < l < -1$ and $\eta_l = +2$ for $-1 < l < l_2$.

This result can be understood in terms of the spectral flow starting from the BEC regime where $\eta_l = 0$. As in the case of the $p+ip$ -wave SF, $\eta_l = 0$ remains valid up to the critical point, since the gap remains open in the entire BEC regime. At the critical point, the gap in the spectrum is minimal at $l = -1$ as shown in Fig. 1 (b), corresponding to the closing of the gap. However, the gap in a finite-size system does not vanish at $l = -1$. As we move into the BCS regime, two non-PHS edge modes develop as in Fig. 2 (a). During this evolution, the Fermi angular momenta evolves from $l = -1$ to non-vanishing values $l_{1,2}$. This induces spectral flow for the angular momenta l in the range $l_1 < l < l_2$, except at $l = -1$. An example of the spectral flow at a fixed value of l is shown in Fig. 2 (c): η_l changes sign exactly when a Fermi angular momentum passes through this l . This picture can be also confirmed in an analytic expression of the edge mode dispersions as functions of $\mu > 0$, as follows [38]. Let us consider the limit of a large disc radius R . The edge of the disc then corresponds to the boundary of a semi-infinite plane, where the momentum parallel to the boundary, k_{\parallel} , is related to the angular momentum l by $k_{\parallel} \simeq l/R$. In the BCS regime $0 < \mu$, the dispersion of the edge modes are given as $E_{\text{edge}}^2 = (\Delta_0^2 \varepsilon_F^2 / (\varepsilon_F^2 + \Delta_0^2)) (2k_{\parallel}^2 / k_F^2 - \mu / \varepsilon_F)^2$ where $\Delta_0 = k_F^2 \Delta$ by solving the BdG equation [38]. The condition $E_{\text{edge}}^2 = 0$ then determines the Fermi wavevector $k_{F\parallel}$ of the edge modes as

$$k_{F\parallel}^2 = \left(\frac{k_F}{\sqrt{2}} \right)^2 \frac{\mu}{\varepsilon_F}. \quad (5)$$

This indeed demonstrates that the Fermi wavevector $k_{F\parallel}$ evolves from zero to a non-vanishing value, as μ is increased from the critical point $\mu = 0$ into the BCS regime.

This confirms the spectral flow for $l_1 < l < l_2$ as found numerically. In fact, spectral flows, and $\eta_l \neq 0$ as a consequence, are common properties of the higher-order pairing states with $\nu \geq 2$ which have non-PHS edge modes in the BCS regime. We have also numerically calculated η_l for $\nu = 3, 4$. As expected, we find $\eta_l = 0$ for all l in the BEC regime. In the BCS regime, on the other hand, there appear ν edge modes: one PHS edge mode and $\nu - 1$ non-PHS edge modes for an odd ν , and ν non-PHS edge modes for an even ν . Let $\{l_j\} (l_j < l_{j+1})$ be Fermi angular momenta for these edge modes, namely the edge modes cross zero energy at $l = l_j$. For $\nu = 3$, we find $\eta_l = \pm 2$ if $|l| < |l_{1,3}|$ and $\eta_l = 0$ otherwise; for $\nu = 4$, $\eta_l = \pm 2$ if $l_{1,3} < l < l_{2,4}$, $\eta_l = \pm 4$ if $l_2 < l < -2$ or $-2 < l < l_3$, and $\eta_l = 0$ otherwise. These results can be naturally understood in terms of the spectral flow starting from $\mu = -\infty$ deep in the BEC regime, as in the case of $\nu = 2$ discussed above. This pattern is expected to persist for any $\nu \geq 2$. To summarize, in general chiral SF with $\nu \geq 2$, η_l changes by ± 2 when a non-PHS edge mode branch crosses zero energy, while a PHS edge mode does not contribute to η_l .

In the BCS regime for $\nu \geq 2$, non-vanishing η_l implies $\mathcal{L}_z \neq 0$. As a consequence, L_z is in fact strongly suppressed from the ‘‘full’’ value $\nu N/2$, in the BCS limit $\Delta_0 = k_F^\nu \Delta \ll \varepsilon_F$. To see this, we evaluate the actual value of \mathcal{L}_z using Eq. (3), with the observations made above. By considering the limit of a large disc, the ‘‘Fermi angular momenta’’ l_j can be written in terms of the Fermi wavenumber parallel to the boundary $k_{F\parallel}^{(j)}$ as $l_j \simeq Rk_{F\parallel}^{(j)}$. Within the quasi-classical formulation, which is legitimate for the BCS limit, we find $\sum_{j=1}^{\nu} (k_{F\parallel}^{(j)})^2 = \nu k_F^2/2$ [38]. Thus, in the leading order in N and Δ_0/ε_F , we obtain

$$\mathcal{L}_z \simeq -\frac{1}{2} \sum_{j=1}^{\nu} l_j^2 = -\frac{1}{2} \sum_{j=1}^{\nu} \left(Rk_{F\parallel}^{(j)} \right)^2 = -\frac{\nu N}{2}. \quad (6)$$

Since $\mathcal{L}_z = L_z - \nu N/2$, the OAM is evaluated to be $L_z = N \times O(\Delta_0/\varepsilon_F)$ in the BCS limit with $\nu \geq 2$, where the $O(\Delta_0/\varepsilon_F)$ term represents possible additional contributions which are beyond the quasi-classical approximation. Indeed, numerical calculations of the OAM give $L_z/N \sim o(0.01)$ when $N \sim O(1000)$ for $\nu = 2, 3, 4$ in an extended range of the BCS regimes with $\Delta_0/\varepsilon_F \lesssim 0.2$, supporting the above quasi-classical analysis. Therefore, the naive evaluation $L_z = \nu N/2$ fails for the chiral SFs in the BCS regime with $\nu \geq 2$, even though it gives the correct value for the $p + ip$ -wave states. That is, L_z is strongly suppressed as if in the naive weak-pairing picture where fermions only near the Fermi surface at $\Delta = 0$ contribute to L_z , but only for $\nu \geq 2$. However, our findings, in particular the stark difference between the $p + ip$ and higher-order ($\nu \geq 2$) pairing cases, make it clear that the suppression cannot be understood by any of the arguments found in existing works. Our analysis

is based on the robustness of the spectral asymmetry η_l , and does not rely on assumptions and approximations used in the earlier papers, such as derivative expansions, which might fail to describe the correct physics especially around boundaries where the edge modes are located [11]. We emphasize that the well-known topological protection of existence of ν edge modes is not sufficient for determining the OAM, which depends on more detailed structures of the edge modes. In this sense, the OAM L_z is a surface-dependent quantity in the BCS regimes.

Finally, let us discuss why the OAM is suppressed for $\nu \geq 2$ but not for $\nu = 1$, in terms of the ground-state wave function. A general expression [38, 39] for the ground state of a BdG Hamiltonian is given as $|\text{GS}\rangle = \mathcal{N}_{\otimes l} |\text{GS}\rangle_l$, where

$$|\text{GS}\rangle_l = \left(\prod_{j=1}^{n_{\uparrow}^{(l)}} \tilde{c}_{j,l+\nu,\uparrow}^{\dagger} \right) \left(\prod_{j=1}^{n_{\downarrow}^{(l)}} \tilde{c}_{j,-l,\downarrow}^{\dagger} \right) \times \exp \left(\sum_{j>n_{\uparrow}^{(l)}} \sum_{j'>n_{\downarrow}^{(l)}} \tilde{c}_{j,l+\nu,\uparrow}^{\dagger} F_{jj'}^{(l)} \tilde{c}_{j',-l,\downarrow}^{\dagger} \right) |0\rangle. \quad (7)$$

Here $|0\rangle$ is the vacuum for $c_{nl\sigma}$ and \mathcal{N} is a normalization constant, $\tilde{c}_{jl\sigma}$ is a linear superposition of $\{c_{nl\sigma}\}_n$, and $n_{\uparrow}^{(l)}, n_{\downarrow}^{(l)}$ are non-negative integers. The ground state of a BdG Hamiltonian is often assumed to have a pure exponential form ($n_{\sigma}^{(l)} = 0$ in Eq. (7)), which implies that all the fermions are paired and thus $L_z = \nu N/2$. For $\nu = 1$, the ground state (of a sufficiently large system) is indeed reduced to the pure exponential form, implying the full OAM $L_z = N/2$. However, the ground state of a BdG Hamiltonian generally takes the form of Eq. (7). A non-vanishing $n_{\sigma}^{(l)}$ signals the existence of *unpaired* fermions, which contribute to the reduction of the OAM.

In fact, we can derive [38] the identity

$$\mathcal{L}_z = -\frac{1}{2} \sum_l \left(l + \frac{\nu}{2} \right) n^{(l)}, \quad n^{(l)} = 2 \left(n_{\downarrow}^{(l)} - n_{\uparrow}^{(l)} \right), \quad (8)$$

which explicitly shows that the unpaired fermions are necessary for the reduction of the OAM, which requires $\mathcal{L}_z \neq 0$. Furthermore, the reduction requires a non-vanishing difference $n_{\uparrow}^{(l)} - n_{\downarrow}^{(l)}$. Indeed, when $n_{\uparrow}^{(l)} = n_{\downarrow}^{(l)}$, $|\text{GS}\rangle$ belongs to the eigenvalue $\mathcal{L}_z = 0$. This is because the vacuum $|0\rangle$ belongs to $\mathcal{L}_z = 0$ and every creation operator in Eq. (7) comes in the pair $\tilde{c}_{l+\nu,\uparrow}^{\dagger} \tilde{c}_{-l,\downarrow}^{\dagger}$, which commutes with $\hat{\mathcal{L}}_z$.

Comparing Eqs. (3) and (8), we obtain $n^{(l)} = \eta_l$. Together with the property $n_{\uparrow}^{(l)} n_{\downarrow}^{(l)} = 0$, we find the numbers of unpaired fermions explicitly as follows [38]: For $\nu = 1$, $n_{\uparrow}^{(l)} = n_{\downarrow}^{(l)} = 0$, namely there is no unpaired fermions as mentioned earlier. For $\nu \geq 2$, $n_{\uparrow}^{(l)} > 0, n_{\downarrow}^{(l)} = 0$ for $l_1 < l < -\nu/2$, and $n_{\uparrow}^{(l)} = 0, n_{\downarrow}^{(l)} > 0$

for $-\nu/2 < l < l_\nu$. Therefore, the unpaired fermions generally carry angular momentum *opposite* to the given chirality, and this contribution cancels out with that from the paired fermions, leading to the reduction of L_z from the full value $\nu N/2$. This depairing effect is associated with the formation of the non-PHS edge modes, signifying the fundamental difference between $\nu = 1$ and $\nu \geq 2$ cases.

We thank Y. Maeno for introducing the problem of the OAM in chiral superfluids to us. We are also grateful to E. Demler, S. Fujimoto, A. Furusaki, J. Goryo, O. Ishikawa, N. Kawakami, Y. B. Kim, T. Kita, T. Mizushima, S.-J. Mao, E.-G. Moon, Y. Nishida, M. Sato, K. Shiozaki, A. Shitade, M. Sigrist, H. Sumiyoshi, W.-F. Tsai, Y. Tsutsumi, K. Ueda, and S.-K. Yip for valuable discussions. This work was supported by the ‘‘Topological Quantum Phenomena’’ (No. 25103706) Grant-in Aid for Scientific Research on Innovative Areas from the Ministry of Education, Culture, Sports, Science and Technology (MEXT) of Japan.

* Corresponding author: wenxing.nie@gmail.com

- [1] D. Vollhart and P. Wölfle, *The Superfluid Phase of Helium 3* (Taylor and Francis, London, 1990), 1st ed.
- [2] M. Ishikawa, *Prog. Theor. Phys.* **57**, 1836 (1977).
- [3] M. G. McClure and S. Takagi, *Phys. Rev. Lett.* **43**, 596 (1979).
- [4] N. D. Mermin and P. Muzikar, *Phys. Rev. B* **21**, 980 (1980).
- [5] G. E. Volovik, *JETP Lett.* **61**, 958 (1995).
- [6] G. E. Volovik, *The Universe in a Helium Droplet* (Oxford University Press, Oxford, 2003).
- [7] A. J. Leggett, *Quantum Liquids: Bose Condensation and Cooper Pairing in Condensed-matter Systems* (Oxford University Press, Oxford, 2006).
- [8] T. Kita, *J. Phys. Soc. Jpn.* **67**, 216 (1998).
- [9] J. Goryo and K. Ishikawa, *Phys. Lett. A* **246**, 549 (1998).
- [10] M. Stone and I. Anduaga, *Ann. Phys.* **323**, 2 (2008).
- [11] J. A. Sauls, *Phys. Rev. B* **84**, 214509 (2011).
- [12] T. Mizushima, M. Ichioka, and K. Machida, *Phys. Rev. Lett.* **101**, 150409 (2008).
- [13] Y. Tsutsumi and K. Machida, *Phys. Rev. B* **85**, 100506(R) (2012).
- [14] B. Bradlyn, M. Goldstein, and N. Read, *Phys. Rev. B* **86**, 245309 (2012).
- [15] C. Hoyos, S. Moroz, and D. T. Son, *Phys. Rev. B* **89**, 174507 (2014).
- [16] A. Shitade and T. Kimura, arXiv:1407.1877.
- [17] P. Anderson and P. Morel, *Phys. Rev.* **123**, 1911 (1961).
- [18] A. J. Leggett, *Rev. Mod. Phys.* **47**, 331 (1975).
- [19] G. E. Volovik, *JETP Lett.* **22**, 108 (1975).
- [20] M. Cross, *J. Low Temp. Phys.* **21**, 525 (1975).
- [21] A. V. Balatsky and V. P. Mineev, *Sov. Phys. JETP* **62**, 1195 (1985).
- [22] A. P. Mackenzie and Y. Maeno, *Rev. Mod. Phys.* **75**, 657 (2003).
- [23] Y. Maeno, S. Kittaka, T. Nomura, S. Yonezawa, and K. Ishida, *J. Phys. Soc. Jpn.* **81**, 011009 (2012).
- [24] H. Ikegami, Y. Tsutsumi, and K. Kono, *Science* **341**, 59 (2013).
- [25] C. R. Hicks, J. R. Kirtley, T. M. Lippman, N. C. Koshnick, M. E. Huber, Y. Maeno, W. M. Yuhasz, M. B. Maple, and K. A. Moler, *Phys. Rev. B* **81**, 214501 (2010).
- [26] M. Z. Hasan and C. L. Kane, *Rev. Mod. Phys.* **82**, 3045 (2010).
- [27] X. L. Qi and S. C. Zhang, *Rev. Mod. Phys.* **83**, 1057 (2011).
- [28] R. Joynt and L. Taillefer, *Rev. Mod. Phys.* **74**, 235 (2002).
- [29] Y. Kasahara, T. Iwasawa, H. Shishido, T. Shibauchi, K. Behnia, Y. Haga, T. D. Matsuda, Y. Onuki, M. Sigrist, and Y. Matsuda, *Phys. Rev. Lett.* **99**, 116402 (2007).
- [30] Y. Nishikubo, K. Kudo, and M. Nohara, *J. Phys. Soc. Jpn.* **80**, 055002 (2011).
- [31] N. Read and D. Green, *Phys. Rev. B* **61**, 10267 (2000).
- [32] A. J. Manninen, T. D. C. Bevan, J. B. Cook, H. Alles, J. R. Hook, and H. E. Hall, *Phys. Rev. Lett.* **77**, 5086 (1996).
- [33] O. Ishikawa (2012), presentation in International Conference on Quantum Fluids and Solids; T. Kunimatsu, H. Nema, M. Kubota, R. Ishiguro, T. Takagi, Y. Sasaki, and O. Ishikawa (2012), presentation in the 67th Annual Japanese Physical Society Meeting.
- [34] M. B. Paranjape, *Phys. Rev. Lett.* **55**, 2390 (1985).
- [35] A. J. Niemi and G. W. Semenoff, *Phys. Rep.* **135**, 99 (1986).
- [36] M. Stone and F. Gaitan, *Ann. Phys.* **178**, 89 (1987).
- [37] J. Yang and C. R. Hu, *Phys. Rev. B* **50**, 16766(R) (1994).
- [38] See supplemental material for details.
- [39] G. Lanboté, *Comm. Math. Phys.* **36**, 59 (1974).

SUPPLEMENTAL MATERIAL

A. Analytic Solution for Edge Modes

Analytic solutions for the edge mode branches on a semi-infinite plane can be obtained by a straightforward calculation. We consider a semi-infinite plane where $y < 0$ is a superfluid region and $y > 0$ is vacuum. Our Hamiltonian for $y < 0$ reads

$$H(k_x) = \begin{bmatrix} (k_x^2 - \partial_y^2)/2m_0 - \mu & \Delta(k_x + \partial_y)^\nu \\ \Delta(k_x - \partial_y)^\nu & -(k_x^2 - \partial_y^2)/2m_0 + \mu \end{bmatrix}. \quad (\text{S1})$$

Analytic properties of a similar Hamiltonian with $\nu = 1$ have been discussed in the context of the topological insulators [1, 2]. We first discuss the $p + ip$ -wave SF and then move to the $d + id$ -wave SF. The edge mode wavefunction u with a boundary condition $u(k_x, y = 0) = 0$ is given by

$$u = \begin{bmatrix} a \\ b \end{bmatrix} (e^{\lambda_1 y} - e^{\lambda_2 y}), \quad (\text{S2})$$

$$\lambda_{1,2}^2 = k_x^2 + 2m_0 \left(\frac{2m_0 \Delta^2}{2} - \mu \right) \pm 2m_0 \sqrt{\left(\frac{2m_0 \Delta^2}{2} - \mu \right)^2 - \mu^2 + E^2}, \quad (\text{S3})$$

where $\text{Re}\lambda_{1,2} > 0$ so that $u(k_x, y \rightarrow -\infty) = 0$. Since $Hu = Eu$, non-zero a, b lead to two equations $(\varepsilon_1 - E)(k_x + \lambda_2) = (\varepsilon_2 - E)(k_x + \lambda_1)$ and $(\varepsilon_1 + E)(k_x - \lambda_2) = (\varepsilon_2 + E)(k_x - \lambda_1)$, where $\varepsilon_{1,2} = (k_x^2 - \lambda_{1,2}^2)/2m_0 - \mu$. By solving these equations, we obtain

$$\lambda_1 + \lambda_2 = 2m_0 E/k_x, \quad (\text{S4})$$

$$\lambda_1 \lambda_2 = 2m_0 \mu - k_x^2. \quad (\text{S5})$$

From Eqs. (S3) and (S5), the edge mode energy is given as

$$[E(k_x)]^2 = \Delta_0^2 k_x^2 / k_F^2. \quad (\text{S6})$$

Note that this is valid only for $\text{Re}\lambda_{1,2} > 0$, or equivalently $k_x^2 < k_F^2 \mu / \varepsilon_F$. From $\lambda_{1,2}$ and E together with the normalization of u , the components of u are determined as $a^2 = b^2 = \Delta_0 / v_F = 1/\xi$ where $v_F = k_F / m_0$.

For the $d + id$ -wave SF, we can compute the edge mode branches in the same way. In this case, $\lambda_{1,2}$ and E are

determined by

$$\lambda_{1,2}^2 = -\frac{\mu/(2m_0)}{[1/(2m_0)]^2 + \Delta^2} + k_x^2 \pm \frac{1}{\sqrt{[1/(2m_0)]^2 + \Delta^2}} \sqrt{\frac{-\mu^2 \Delta^2}{[1/(2m_0)]^2 + \Delta^2} + E^2}, \quad (\text{S7})$$

$$\lambda_1 + \lambda_2 = \frac{2k_x E}{2k_x^2/(2m_0) - \mu}, \quad (\text{S8})$$

$$\lambda_1 \lambda_2 = 2m_0 \mu + \frac{2m_0 E^2}{2k_x^2/(2m_0) - \mu} - k_x^2. \quad (\text{S9})$$

From these equations, we obtain

$$[E_{1,2}(k_x)]^2 = \frac{\Delta_0^2 \varepsilon_F^2}{\varepsilon_F^2 + \Delta_0^2} \left(2 \frac{k_x^2}{k_F^2} - \frac{\mu}{\varepsilon_F} \right)^2. \quad (\text{S10})$$

The above E is reduced to the well-known quasi-classical result $E_{1,2}^2 = \Delta_0^2 (2k_x^2/k_F^2 - 1)^2$ when $\mu = \varepsilon_F \gg \Delta_0$ [3]. The components $a_{1,2}, b_{1,2}$ are the solutions of

$$a_j^2 + b_j^2 = \frac{2\Delta_0 |k_x|}{\sqrt{\varepsilon_F^2 + \Delta_0^2}} \frac{\mu \varepsilon_F - (\varepsilon_F^2 - \Delta_0^2) k^2 / k_F^2}{\mu \varepsilon_F - (\varepsilon_F^2 + \Delta_0^2) k^2 / k_F^2}, \quad (\text{S11})$$

$$\frac{a_1^2}{b_1^2} = \frac{\varepsilon_F^2 + \Delta_0^2}{\varepsilon_F^2} \left(1 + \frac{\Delta_0}{\sqrt{\varepsilon_F^2 + \Delta_0^2}} \right)^2, \quad (\text{S12})$$

$$\frac{a_2^2}{b_2^2} = \frac{\varepsilon_F^2 + \Delta_0^2}{\varepsilon_F^2} \left(1 - \frac{\Delta_0}{\sqrt{\varepsilon_F^2 + \Delta_0^2}} \right)^2. \quad (\text{S13})$$

It is easy to check $a_1^2 = b_2^2$ and $b_1^2 = a_2^2$ which are implied from the particle-hole symmetry of the Hamiltonian, $PH(k_x)P^{-1} = -H(-k_x)$ with $P = i\sigma_y$. Note that k_x is restricted to $0 < k_x^2 < k_F^2 \mu \varepsilon_F / (\varepsilon_F^2 + \Delta_0^2)$ from the condition $\text{Re}\lambda_{1,2} > 0$ and Eq. (S11). In the quasi-classical limit, a_j, b_j are simply reduced to $a_j^2 = b_j^2 = 2|k_x|/\xi k_F$.

B. Quasi-Classical Calculation of \mathcal{L}_z

Here, we discuss \mathcal{L}_z in the quasi-classical limit $\Delta_0 = k_F^\nu \Delta \ll \varepsilon_F$ in the BCS regimes. First, as we discussed in the main text and saw in Fig. 2 (b), η_l changes ± 2 only when a non-PHS edge mode branch crosses zero energy as a function of l , which is confirmed numerically. Therefore, we simply count how many times the non-PHS edge mode branches cut zero energy, and obtain

$$\eta_l = -2 \sum_{j=1}^{\lfloor \nu/2 \rfloor} \theta(l - l_j) \quad (\text{S14})$$

for $l < -\nu/2$, where l_j is the ‘‘Fermi angular momenta’’ at which j -th edge mode branch crosses zero energy as

a function of l and $\theta(l - l_j)$ is the step function. We have labeled the edge modes so that $l_1 < l_2 < \dots < l_\nu$ is satisfied. $\eta_l = -\eta_{-l-\nu}$ holds for $l > -\nu/2$ by the particle-hole symmetry. By using this, we obtain

$$\begin{aligned} \mathcal{L}_z &= -\frac{1}{2} \times 2 \sum_{j=1}^{\lfloor \nu/2 \rfloor} 2 \times \frac{1}{2} (l_j + \nu/2)(l_j + \nu/2 - 1) \\ &\simeq -\frac{1}{2} \sum_{j=1}^{\nu} l_j^2 \end{aligned} \quad (\text{S15})$$

for even ν s. In the second equality, we neglected $o(l_j)$ contributions which is much smaller than the l_j^2 -contributions when the total number of fermions N is large enough. Contributions from $l > -\nu/2$ has been included by introducing a factor 2 in front of the summation $\sum_{j=1}^{\lfloor \nu/2 \rfloor}$. Equation (S15) also holds for odd ν s.

The Fermi angular momentum $\{l_j\}$ of the edge modes are evaluated within quasi-classical calculations. When the radius of the system is large, $\xi = v_F/\Delta_0 \ll R \rightarrow \infty$, curvature of the boundary could be negligible and the physics around the boundary would be equivalent to that in a cylinder system or a semi-infinite system. In such systems, edge mode wavefunctions are proportional to $\exp[ik_{\parallel}x_{\parallel}]$ where $k_{\parallel}, x_{\parallel}$ are a wavenumber and a position along the boundary, respectively. Since the edge modes are well localized around the boundary, we can regard the edge modes as running at the boundary $r = R$ in the disc geometry. In this case, the (anti-)periodic boundary condition is satisfied, $k_{\parallel} \simeq 2\pi l/(2\pi R) = l/R$. Especially, the Fermi angular momentum $\{l_j\}$ of the edge modes are connected with their Fermi wavenumbers $\{k_{F\parallel}^{(j)}\}$ as

$$l_j \simeq Rk_{F\parallel}^{(j)}. \quad (\text{S16})$$

Therefore, we obtain a quasi-classical expression for \mathcal{L}_z ,

$$\mathcal{L}_z \simeq -\frac{1}{2} \sum_{j=1}^{\nu} (Rk_{F\parallel}^{(j)})^2. \quad (\text{S17})$$

The Fermi wavenumbers $\{k_{F\parallel}^{(j)}\}$ can easily be calculated for semi-infinite systems within the quasi-classical calculations. Let us assume that the system has a straight boundary along y -axis at $x = 0$ which separates the SF in $x < 0$ from the vacuum in $x > 0$. By solving the BdG equation near the boundary, we obtain an equation which determines the edge mode energy E [3],

$$\frac{\Delta_+}{E - i\sqrt{|\Delta_+|^2 - E^2}} = \frac{\Delta_-}{E + i\sqrt{|\Delta_-|^2 - E^2}}. \quad (\text{S18})$$

Here, we have defined $\Delta_{\pm} = \Delta_0(\pm k_x + ik_y)^{\nu}/k_F^{\nu}$ with $k_x = \sqrt{k_F^2 - k_y^2}$. If we rewrite $\Delta_+ = \Delta_{\text{odd}} + \Delta_{\text{even}}$ where $\Delta_{\text{odd/even}}$ are odd/even with respect to $k_x \leftrightarrow -k_x$, the above equation leads to $\Delta_{\text{even}} = 0$ at the Fermi

wavenumber of the one dimensional edge modes where $E = 0$. By using $k_x = k_F \cos \theta, k_y = k_F \sin \theta$, it is seen that $\Delta_{\text{even}} = \Delta_0 \cos(\nu\theta)$ for an even ν , and $\Delta_{\text{even}} = i\Delta_0 \sin(\nu\theta)$ for an odd ν .

Then, we can evaluate the Fermi wavenumbers of the ν edge modes along the y -direction. It is written as $k_{F\parallel}^{(j)} = k_F \sin \theta_F^{(j)}$ where $\theta_F^{(j)} = -\pi/2 + (2j - 1)\pi/2\nu$ for $j = 1, \dots, \nu$ satisfying $\Delta_{\text{even}}(\theta_F^{(j)}) = 0$. For $\nu \geq 2$, since $\sum_{j=1}^{\nu} e^{i(2j-1)\pi/\nu} = 0$, we obtain an identity within the quasi-classical calculation,

$$\begin{aligned} \sum_{j=1}^{\nu} \left(k_{F\parallel}^{(j)}\right)^2 &= \sum_{j=1}^{\nu} k_F^2 [\sin(\theta_F^{(j)})]^2 \\ &= k_F^2 \sum_{j=1}^{\nu} \left(\frac{1}{2} - \frac{\cos(2\theta_F^{(j)})}{2}\right) \\ &= \nu \frac{k_F^2}{2}. \end{aligned} \quad (\text{S19})$$

There would be possible deviations of $k_{F\parallel}^{(j)}$ from the above values, which are beyond the present quasi-classical approximation. From Eq. (S19), we obtain the same identity for the perpendicular component $k_{F\perp}^{(j)} = k_F \cos \theta_F^{(j)}$,

$$\sum_{j=1}^{\nu} \left(k_{F\perp}^{(j)}\right)^2 = \nu \frac{k_F^2}{2}. \quad (\text{S20})$$

These equations are a direct consequence of the residual ν -hold rotational symmetry of the gap function. The condition $\Delta_{\text{even}} = 0$ means vanishing edge mode energy $E = 0$ when the two-dimensional wavenumber $(k_{F\perp}^{(j)}, k_{F\parallel}^{(j)})$ is at nodes of Δ_{even} , where positions of the nodes are ν -hold rotationally symmetric. This symmetry immediately leads to $\sum_{j=1}^{\nu} (k_{F\perp}^{(j)})^2 = \sum_{j=1}^{\nu} (k_{F\parallel}^{(j)})^2$, from which we can easily reproduce Eqs. (S19) and (S20) since the wavenumber is on the two-dimensional Fermi surface, $[(k_{F\perp}^{(j)})^2 + (k_{F\parallel}^{(j)})^2] = k_F^2$ for each j within the quasi-classical calculation. On the other hand, for $\nu = 1$, there is no residual rotational symmetry in Δ_{even} . This explains the difference between $\nu = 1$ and $\nu \geq 2$.

We can see that Eqs. (S19) and (S20) are indeed satisfied by directly looking at $k_{F\parallel}^{(j)}$; $|k_{F\parallel}^{(j)}| = k_F/\sqrt{2} \simeq 0.71k_F$ for $\nu = 2$, $|k_{F\parallel}^{(j)}| = 0, \sqrt{3}k_F/2 \simeq 0.87k_F$ for $\nu = 3$, and $|k_{F\parallel}^{(j)}| = k_F\sqrt{1/2 \pm 1/2\sqrt{2}} \simeq 0.93k_F, 0.38k_F$ for $\nu = 4$, and so on. We have numerically confirmed that Eq. (S19) holds also for the disc geometry. For example, when $k_FR = 80$, the edge mode Fermi wavenumbers are numerically obtained as $|k_{F\parallel}^{(1,2)}| \simeq 56k_F/80 \simeq 0.70k_F$ for $\nu = 2$, $|k_{F\parallel}^{(1,3)}| \simeq 68k_F/80 \simeq 0.85k_F, |k_{F\parallel}^{(2)}| \simeq 1k_F/80 \simeq 0.013k_F$ for $\nu = 3$, and $|k_{F\parallel}^{(1,4)}| \simeq 72k_F/80 \simeq 0.90k_F, |k_{F\parallel}^{(2,3)}| \simeq 31k_F/80 \simeq 0.39k_F$ for $\nu = 4$ for several values of $\Delta_0 \ll \varepsilon_F$. We note that, although the above discussions

are not based on self-consistent calculations, Eq. (S19) should be satisfied even in self-consistent calculations for the BCS limit, since $\{k_{F\parallel}^{(j)}\}$ are generally determined by symmetry of the gap functions.

When μ and Δ are tuned so that N is fixed, the total number of fermions on the disc is expressed as

$$N \simeq V n_{2D} = R^2 k_F^2 / 2, \quad (\text{S21})$$

where $n_{2D} = k_F^2 / 2\pi$ is the particle density in two dimensions and $V = \pi R^2$ is the volume of the system. We have neglected $o(R)$ contributions which can arise from deviations of the particle density from n_{2D} near the boundary. From Eqs. (S17), (S19), and (S21), we obtain Eq. (6) in the main text.

C. Ground State Wavefunctions

A general theory of the Bogoliubov transformation was developed in Ref. [4]. We follow it and obtain the ground state wavefunctions for the chiral SFs on the disc. The Bogoliubov transformation is introduced as

$$\begin{bmatrix} c_{nl+\nu\uparrow} \\ c_{n-l\downarrow}^\dagger \end{bmatrix} = \sum_{m=1}^M \begin{bmatrix} u_{nm}^{(l)} & u_{nM+m}^{(l)} \\ v_{nm}^{(l)} & v_{nM+m}^{(l)} \end{bmatrix} \begin{bmatrix} b_m^{(l)} \\ b_{M+m}^{(l)} \end{bmatrix}, \quad (\text{S22})$$

where $(u, v)^T$ are eigenvectors of the BdG equation,

$$\sum_{n'=1}^M \left(H_{\text{BdG}}^{(l)} \right)_{nn'} \begin{bmatrix} u_{n'm}^{(l)} \\ v_{n'm}^{(l)} \end{bmatrix} = E_m^{(l)} \begin{bmatrix} u_{nm}^{(l)} \\ v_{nm}^{(l)} \end{bmatrix}. \quad (\text{S23})$$

We have introduced the cut-off $M \gg 1$ as in the main text. The ground state |GS⟩ is defined as a vacuum for all the quasi-particle excitations with positive energies,

$$\begin{cases} b_m^{(l)} |\text{GS}\rangle = 0 & (E_m^{(l)} > 0), \\ b_m^{(l)\dagger} |\text{GS}\rangle = 0 & (E_m^{(l)} < 0). \end{cases} \quad (\text{S24})$$

Let the number of the positive (negative) eigenvalues of $H_{\text{BdG}}^{(l)}$ be $n_+^{(l)} (n_-^{(l)})$ which are $n_+^{(l)} \neq n_-^{(l)}$ in general, and we label the eigenvalues so that $E_1^{(l)} \geq \dots \geq E_{2M}^{(l)}$. Correspondingly, the b -operators are rewritten as $b_{m+}^{(l)} \equiv b_m^{(l)}$ for $E_m^{(l)} > 0$ and $b_{m-}^{(l)} \equiv b_m^{(l)\dagger}$ for $E_m^{(l)} < 0$. We also rewrite the unitary matrix for the transformation as,

$$U^{(l)} \equiv \begin{bmatrix} u_{nm}^{(l)} & u_{nM+m}^{(l)} \\ v_{nm}^{(l)} & v_{nM+m}^{(l)} \end{bmatrix}^{-1} = \begin{bmatrix} U_1^{(l)} & U_2^{(l)} \\ U_3^{(l)} & U_4^{(l)} \end{bmatrix}, \quad (\text{S25})$$

where sizes of the matrices are $n_+^{(l)} \times M$ for $U_{1,2}$ and $n_-^{(l)} \times M$ for $U_{3,4}$.

Since $U_3^{(l)\dagger} U_3^{(l)}$ is an $M \times M$ Hermitian matrix, it has real eigenvalues $\{\lambda_{3j}^{(l)}\}_{j=1}^M$ with eigenvectors $\{X_{3j}^{(l)}\}_{j=1}^M$,

$$\left(U_3^{(l)\dagger} U_3^{(l)} \right) X_{3j}^{(l)} = \lambda_{3j}^{(l)} X_{3j}^{(l)}. \quad (\text{S26})$$

We denote the number of $\lambda_{3j}^{(l)} = 1$ as $n_+^{(l)} \geq 0$. $U_3^{(l)} U_3^{(l)\dagger}$ is a $n_-^{(l)} \times n_-^{(l)}$ Hermitian matrix and has real eigenvalues $\{\lambda_{1j}^{(l)}\}_{j=1}^{n_-^{(l)}}$ with eigenvectors $\{X_{1j}^{(l)}\}_{j=1}^{n_-^{(l)}}$. Similarly, an $M \times M$ Hermitian matrix $U_2^{(l)\dagger} U_2^{(l)}$ has real eigenvalues $\{\lambda_{2j}^{(l)}\}_{j=1}^M$ with eigenvectors $\{X_{2j}^{(l)}\}_{j=1}^M$, and a $n_+^{(l)} \times n_+^{(l)}$ Hermitian matrix $U_2^{(l)} U_2^{(l)\dagger}$ has real eigenvalues $\{\lambda_{4j}^{(l)}\}_{j=1}^{n_+^{(l)}}$ with eigenvectors $\{X_{4j}^{(l)}\}_{j=1}^{n_+^{(l)}}$. We denote the number of $\lambda_{2j}^{(l)} = 1$ as $n_-^{(l)} \geq 0$.

We then define new fermionic operators,

$$\begin{cases} \tilde{c}_{jl\uparrow} = \sum_{n=1}^M X_{3jn}^{(l)*} c_{nl\uparrow} & (j = 1, \dots, M), \\ \tilde{c}_{jl\downarrow}^\dagger = \sum_{n=1}^M X_{2jn}^{(l)} c_{nl\downarrow}^\dagger & (j = 1, \dots, M), \\ \tilde{b}_{j+}^{(l)} = \sum_{j=1}^{n_+^{(l)}} X_{4jm}^{(l)*} b_{m+}^{(l)} & (j = 1, \dots, n_+^{(l)}), \\ \tilde{b}_{j-}^{(l)\dagger} = \sum_{j=1}^{n_-^{(l)}} X_{1jm}^{(l)} b_{m-}^{(l)\dagger} & (j = 1, \dots, n_-^{(l)}). \end{cases} \quad (\text{S27})$$

The above transformations can be implemented by a unitary operator $\mathcal{U}^{(l)}$ which transforms the \tilde{c} operators as

$$\begin{cases} \mathcal{U}^{(l)\dagger} \tilde{c}_{jl\uparrow} \mathcal{U}^{(l)} = \tilde{b}_{j-}^{(l)} & (j = 1, \dots, n_+^{(l)}), \\ \mathcal{U}^{(l)\dagger} \tilde{c}_{n_+^{(l)}+j,l\uparrow} \mathcal{U}^{(l)} = \tilde{b}_{n_+^{(l)}+j,+}^{(l)} & (j = 1, \dots, M - n_+^{(l)}), \\ \mathcal{U}^{(l)\dagger} \tilde{c}_{jl\downarrow} \mathcal{U}^{(l)} = \tilde{b}_{j+}^{(l)} & (j = 1, \dots, n_-^{(l)}), \\ \mathcal{U}^{(l)\dagger} \tilde{c}_{n_-^{(l)}+j,l\downarrow} \mathcal{U}^{(l)} = \tilde{b}_{n_-^{(l)}+j,-}^{(l)} & (j = 1, \dots, M - n_-^{(l)}). \end{cases} \quad (\text{S28})$$

An explicit form of the unitary operator $\mathcal{U}^{(l)}$ is found in Ref. [4]. By definition, $M \mp n_{\pm}^{(l)} \pm n_{\pm}^{(l)} = n_{\pm}^{(l)}$, i.e. $\eta_{\pm} = n_{\pm}^{(l)} - n_{\mp}^{(l)} = 2(n_{\downarrow}^{(l)} - n_{\uparrow}^{(l)}) = n^{(l)}$, are satisfied in the transformation. The ground state wavefunction is now obtained as $|\text{GS}\rangle = \mathcal{N} \otimes_l |\text{GS}\rangle_l$, where

$$\begin{aligned} |\text{GS}\rangle_l &= \mathcal{U}^{(l)\dagger} |0\rangle \\ &\propto \left(\prod_{j=1}^{n_+^{(l)}} \tilde{c}_{j,l+\nu,\uparrow}^\dagger \right) \left(\prod_{j=1}^{n_-^{(l)}} \tilde{c}_{j,-l,\downarrow} \right) \\ &\times \exp \left(\sum_{j>n_+^{(l)}}^M \sum_{j'>n_-^{(l)}}^M \tilde{c}_{j,l+\nu,\uparrow}^\dagger F_{jj'}^{(l)} \tilde{c}_{j',-l,\downarrow} \right) |0\rangle. \end{aligned} \quad (\text{S29})$$

The coefficients $F_{jj'}^{(l)}$ are the solution of

$$\sum_{j>n_+^{(l)}}^M \left(X_{4j'}^{(l)} U_1^{(l)} X_{3j}^{(l)} \right) F_{jj''}^{(l)} = -X_{4j'}^{(l)} U_2^{(l)} X_{2j''}^{(l)} \quad (\text{S30})$$

for $j', j'' > n_{\downarrow}^{(l)}$. It is noted that at least one of $n_{\uparrow}^{(l)}$ or $n_{\downarrow}^{(l)}$ must be zero in our Hamiltonian, because the present gap functions are “nodeless”. In order to see

this, we first divide the Hamiltonian as $H = \sum_{lj} h_{jj'}^{(l)} = \sum_l (H_1^{(l)} + H_2^{(l)} + H_{12}^{(l)})$, where

$$h_{jj'}^{(l)} = \begin{bmatrix} \tilde{c}_{jl+\nu\uparrow}^\dagger \\ \tilde{c}_{j-l\downarrow} \end{bmatrix} \tilde{H}_{\text{BdG}jj'}^{(l)} \begin{bmatrix} \tilde{c}_{j'l+\nu\uparrow} \\ \tilde{c}_{j'-l\downarrow}^\dagger \end{bmatrix}, \quad (\text{S31})$$

$$\tilde{H}_{\text{BdG}}^{(l)} = \begin{bmatrix} X_3^{(l)*} & 0 \\ 0 & X_2^{(l)} \end{bmatrix}^\dagger H_{\text{BdG}}^{(l)} \begin{bmatrix} X_3^{(l)*} & 0 \\ 0 & X_2^{(l)} \end{bmatrix}$$

$$= \begin{bmatrix} \tilde{\varepsilon}^{(l)} & \tilde{\Delta}^{(l)} \\ \tilde{\Delta}^{(l)\dagger} & -\tilde{\varepsilon}'^{(l)} \end{bmatrix}. \quad (\text{S32})$$

Each of $H_\alpha^{(l)}$ ($\alpha = 1, 2, 12$) consists of some combinations of $c_j^\dagger c_{j'}$, $c_j^\dagger c_{j'}^\dagger$, and $c_j c_{j'}$. $H_1^{(l)}$ includes the \tilde{c} -operators only for $j, j' = 1, \dots, n_{\uparrow,\downarrow}^{(l)}$, while $H_2^{(l)}$ has the \tilde{c} -operators only for $j, j' = n_{\uparrow,\downarrow}^{(l)}, \dots, M$. $H_{12}^{(l)}$ connects the two sectors. Since $|\text{GS}\rangle_l$ is partly diagonal in the j -space, the off-diagonal part vanishes $H_{12}^{(l)}|\text{GS}\rangle_l = 0$. Therefore, $H_{1,2}|\text{GS}\rangle_l \propto |\text{GS}\rangle_l$ should be satisfied for each $i = 1, 2$. Here, let us assume that both of $n_{\uparrow}^{(l)}$ and $n_{\downarrow}^{(l)}$ are non-zero. Then, from $H_1|\text{GS}\rangle_l \propto |\text{GS}\rangle_l$, we see that $\tilde{\Delta}_{jj'}^{(l)\dagger} = 0$ for $j = 1, \dots, n_{\downarrow}^{(l)}$ and $j' = 1, \dots, n_{\uparrow}^{(l)}$. Similarly, from $H_{12}|\text{GS}\rangle_l \propto |\text{GS}\rangle_l$, it is seen that $\tilde{\Delta}_{jj'}^{(l)\dagger} = 0$ for $j = n_{\downarrow}^{(l)} + 1, \dots, M$ and $j' = 1, \dots, n_{\uparrow}^{(l)}$, and $\tilde{\Delta}_{jj'}^{(l)\dagger} = 0$ for $j = n_{\uparrow}^{(l)} + 1, \dots, M$ and $j' = 1, \dots, n_{\downarrow}^{(l)}$. This means that $\tilde{\Delta}^{(l)}$ is not invertible, and $\Delta^{(l)} = X_2^{(l)T} \tilde{\Delta}^{(l)} X_3^{(l)}$ is also non-invertible. Therefore, $\Delta^{(l)\dagger} \Delta^{(l)}$ must have an eigenvector with zero-eigenvalue. Since this matrix is a representation of the Hermitian operator $\Delta^2(\partial_x^2 + \partial_y^2)^\nu$ on $L^2([0, R] \times [0, 2\pi))$ with the Dirichlet boundary condition $\psi(r = R) = 0$, $\Delta^2(\partial_x^2 + \partial_y^2)^\nu$ also must have a zero-eigenvalue. However, since Laplacian is positive definite on $L^2([0, R] \times [0, 2\pi))$, $\Delta^{(l)\dagger} \Delta^{(l)}$ does not have an eigenvector with zero-eigenvalue, which means that $\Delta^{(l)}$ and $\tilde{\Delta}^{(l)} = X_3^{(l)T} \Delta^{(l)} X_2^{(l)}$ are invertible. Because the resulting non-invertibility of $\tilde{\Delta}^{(l)}$ under the above assumption contradicts with this, at least one of $n_{\uparrow}^{(l)}$ or $n_{\downarrow}^{(l)}$ must be zero. This is reasonable since it can be considered that the factor $\prod(\tilde{c}_{l+1\uparrow}^\dagger \tilde{c}_{-l\downarrow}^\dagger)$ corresponds to nodes of gap functions, which is seen in the ground state for nodal SFs under the periodic boundary condition, $|\text{nodal}\rangle \propto \prod_{k:\Delta_k=0, k < k_F} c_{k\uparrow}^\dagger c_{-k\downarrow}^\dagger \prod_{k:\Delta_k \neq 0} \exp(-v_k/u_k c_{k\uparrow}^\dagger c_{-k\downarrow}^\dagger) |0\rangle$, where $(u_k, v_k)^T$ are the eigenvectors of the BdG equation. We can evaluate $\hat{\mathcal{L}}_z$ within the present scheme, either by using the relation $n_{\uparrow}^{(l)} - n_{\downarrow}^{(l)} = 2(n_{\downarrow}^{(l)} - n_{\uparrow}^{(l)})$ or by directly using the explicit expression of $|\text{GS}\rangle$. Then, it is

confirmed that Eq. (3) and Eq. (8) in the main text are indeed equivalent. This equivalence is used in order to determine $n_{\uparrow,\downarrow}^{(l)}$ in the following.

In the $p + ip$ -wave SF, $\eta_l = 0$ for all l both in the BEC regime and the BCS regime. Therefore, the ground state wavefunction has only the exponential factor and is given by, for any μ ,

$$|p\text{GS}\rangle_l = \exp[\tilde{c}_{l+1}^\dagger F^{(l)} \tilde{c}_{-l}^\dagger] |0\rangle. \quad (\text{S33})$$

For simplicity, we have suppressed the indices j, σ . Similarly, in the BEC regimes with $\nu \geq 2$, since $\eta_l = 0$ holds, $n_{\uparrow}^{(l)} = n_{\downarrow}^{(l)} = 0$ and the ground state wavefunctions are simply of the exponential forms. However, in the BCS regimes with $\nu \geq 2$, there exist the factor $\prod \tilde{c}_{l+\nu\uparrow}^\dagger$ or $\prod \tilde{c}_{-l\downarrow}^\dagger$. Since $n_{\uparrow,\downarrow}^{(l)} \geq 0$ and $n_{\uparrow}^{(l)} n_{\downarrow}^{(l)} = 0$, we can determine each of them from the relation $\eta_l = n_{\uparrow}^{(l)} - n_{\downarrow}^{(l)} = 2(n_{\downarrow}^{(l)} - n_{\uparrow}^{(l)}) = n^{(l)}$. For the $d + id$ -wave states, since $\eta_l = -2$ for $l_1 < l < -1$, we have $n_{\uparrow}^{(l)} = 1$ and $n_{\downarrow}^{(l)} = 0$ there. Similarly, since $\eta_l = +2$ for $-1 < l < l_2$, we have $n_{\uparrow}^{(l)} = 0$ and $n_{\downarrow}^{(l)} = 1$. Hence, the ground state wavefunction is given by

$$|d\text{GS}\rangle_l = \begin{cases} \exp[\tilde{c}_{l+2}^\dagger F^{(l)} \tilde{c}_{-l}^\dagger] |0\rangle & (|l| > |l_{1,2}|, l = -1), \\ \tilde{c}_{l+2}^\dagger \exp[\tilde{c}_{l+2}^\dagger F^{(l)} \tilde{c}_{-l}^\dagger] |0\rangle & (l_1 < l < -1), \\ \tilde{c}_{-l}^\dagger \exp[\tilde{c}_{l+2}^\dagger F^{(l)} \tilde{c}_{-l}^\dagger] |0\rangle & (-1 < l < l_2). \end{cases} \quad (\text{S34})$$

We note that, $c_{n,l+2}(c_{n,-l})$ -fermions have lower energies than $c_{n,-l}(c_{n,l+2})$ -fermions with the same radial quantum number n for $-l_1 < l < -1$ ($-1 < l < l_2$). This would be the reason why the $\tilde{c}_{l+2}(\tilde{c}_{-l})$ -fermions are unpaired for $-l_1 < l < -1$ ($-1 < l < l_2$), but not vice versa. Similar wavefunctions with unpaired fermions represented by extra $\tilde{c}_{l+\nu}^\dagger, \tilde{c}_{-l}^\dagger$ operators are also obtained for $\nu \geq 3$ in the BCS regimes.

* Corresponding author: wenxing.nie@gmail.com

- [S1] B. Zhou, H. -Z. Lu, R. -L. Chu, S. -Q. Shen, and Q. Niu, Phys. Rev. Lett. **101**, 246807 (2008).
[S2] M. Wada, S. Murakami, F. Freimuth, G. Bihlmayer, Phys. Rev. B **83**, 121310(R) (2011).
[S3] J. Yang and C. -R. Hu, Phys. Rev. B **50**, 16766(R) (1994).
[S4] G. Lanboté, Comm. Math. Phys. **36**, 59 (1974).